

additional databases **18** and **19** (Scheme 4) to establish the complete structure of the desertomycin/oasomycin class of natural products.

Received: August 8, 2000 [Z15604]

- [1] Y. Kobayashi, C.-H. Tan, Y. Kishi, *Angew. Chem.* **2000**, *112*, 4449; *Angew. Chem. Int. Ed.* **2000**, *39*, 4279.
- [2] The degradation product **2b** was also obtained from oasomycin B in five steps: 1) O<sub>3</sub>/MeOH/−78°C; 2) NaBH<sub>4</sub>/MeOH/RT; 3) Ac<sub>2</sub>O/Py; 4) EtSH/conc. HCl; 5) Ac<sub>2</sub>O/Py.
- [3] We thank Dr. Gerhard Kretzschmar for samples of oasomycins A and B.
- [4] a) H. C. Brown, K. S. Bhat, *J. Am. Chem. Soc.* **1986**, *108*, 5919; b) H. C. Brown, K. S. Bhat, R. S. Randad, *J. Org. Chem.* **1989**, *54*, 1570.
- [5] Y. Kobayashi, J. Lee, K. Tezuka, Y. Kishi, *Org. Lett.* **1999**, *1*, 2177.
- [6] The enantiomeric excess was estimated from the <sup>19</sup>F NMR spectrum of its (*R*)-Mosher ester.
- [7] The minor product was removed by column chromatography on silica gel.
- [8] a) S. D. Rychnovsky, D. J. Skalitzy, *Tetrahedron Lett.* **1990**, *31*, 945; b) D. A. Evans, D. L. Reiger, J. R. Gage, *Tetrahedron Lett.* **1990**, *31*, 7099.
- [9] E. J. Corey, P. D. Jardine, S. Virgil, P.-W. Yuen, R. D. Connell, *J. Am. Chem. Soc.* **1989**, *111*, 9243.
- [10] Dihydroxylation of **9** in the presence of the Corey (*S,S*)-ligand gave a 1:7 mixture of the two diols.
- [11] The dithiane **11** was prepared from L-(+)-arabinose. By using Gray's procedure (M. Y. H. Wong, G. R. Gray, *J. Am. Chem. Soc.* **1978**, *100*, 3548), L-(+)-arabinose was transformed to the diethylthioacetal, corresponding to structure **4** in Gray's paper. This diethylthioacetal was then subjected to the following three steps: 1) TBDPSCl, imidazole, DMF, RT; 2) HgO, HgCl<sub>2</sub>, acetone/H<sub>2</sub>O (10/1), RT; 3) 1,3-propanedithiol, BF<sub>3</sub>·OEt<sub>2</sub>, CH<sub>2</sub>Cl<sub>2</sub>, 0°C (26% overall yield from L-(+)-arabinose).
- [12] D. A. Evans, K. T. Chapman, E. M. Carreira, *J. Am. Chem. Soc.* **1988**, *110*, 3560.
- [13] Acetonization (MeC(OMe)<sub>2</sub>Me, acetone, CSA) of **13** yielded an approximately 1:1:1 mixture of the acetonides. The acetonide **d** was isolated in a pure form by chromatography on silica gel.
- [14] **2b** (synthetic): <sup>1</sup>H NMR (500 MHz, CDCl<sub>3</sub>): see Figure 1; <sup>13</sup>C NMR (100 MHz, CDCl<sub>3</sub>): δ = 9.4, 10.7, 20.8–21.2 (overlapped), 34.8, 35.5, 36.6, 37.0, 37.3, 37.6, 39.1, 61.9, 65.1, 65.6, 67.1, 67.2, 67.6, 67.9, 71.5, 71.6, 71.8, 77.2, 169.9–170.5 (overlapped); [α]<sub>D</sub><sup>20</sup> = +5.7 (*c* = 0.23 in MeOH). **2b** (natural): <sup>1</sup>H NMR (500 MHz, CDCl<sub>3</sub>): see Figure 1; <sup>13</sup>C NMR (100 MHz, CDCl<sub>3</sub>): identical to synthetic **2b**; [α]<sub>D</sub><sup>20</sup> = +7.8 (*c* = 0.25 in MeOH).
- [15] Oasomycins A and B are known to exhibit significant differences in the chemical shifts of the carbon atoms and protons at the C20–C23 region; see the structures in Scheme 1 and the references quoted in A. Bax, A. Aszalos, Z. Dinya, K. Sudo, *J. Am. Chem. Soc.* **1986**, *108*, 8056 and S. Grabley, G. Kretzschmar, M. Mayer, S. Philipps, R. Thiericke, J. Wink, A. Zeeck, *Liebigs Ann. Chem.* **1993**, 573.
- [16] Abbreviations: Ac = acetyl; Bu = butyl; Bn = benzyl; CSA = 10-camphorsulfonic acid; DMAP = 4-dimethylaminopyridine; DDQ = 2,3-dichloro-5,6-dicyano-1,4-benzoquinone; DMF = *N,N*-dimethylformamide; DMP = Dess–Martin periodinane; DMSO = dimethylsulfoxide; Ipc = isopinocampheyl; MPM = 4-methoxyphenylmethyl; NMO = *N*-methylmorpholine *N*-oxide; Piv = pivaloyl = trimethylacetyl; Py = pyridine; TBS = *tert*-butyldimethylsilyl; TBDPS = *tert*-butyldiphenylsilyl; THF = tetrahydrofuran; Ts = toluene-4-sulfonyl.

## Tuning the Regiospecificity of Cleavage in Fe<sup>III</sup> Catecholate Complexes: Tridentate Facial versus Meridional Ligands\*\*

Du-Hwan Jo and Lawrence Que, Jr.\*

Bacterial catechol dioxygenases are a component of nature's strategy for degrading aromatic molecules to aliphatic products in the environment.<sup>[1]</sup> These enzymes catalyze the oxidative cleavage of catechols, which leads to the scission of the C1–C2 (intradiol) or C2–C3 (extradiol) bond. Intradiol-cleaving enzymes have an iron(III) active site, while extradiol-cleaving enzymes require Fe<sup>II</sup> or Mn<sup>II</sup>.<sup>[1, 2]</sup> To date the factors that determine the regiospecificity of cleavage are not well understood. Most biomimetic studies have focused on iron(III) catecholate complexes with tetradentate ligands, all of which performed only intradiol cleavage.<sup>[3]</sup> However, the few examples of iron(III) catecholate complexes having tridentate ligands result in at least some extradiol cleavage products.<sup>[4]</sup> To further investigate the factors that determine the cleavage site, we characterized a series of mononuclear iron(III) catecholate complexes [(L)Fe(DBC)Cl] [L = Me<sub>3</sub>-TACN (**1**), TPY (**2**), BnBPA (**3**)],<sup>[5]</sup> containing tridentate ligands that can coordinate the metal center in a facial or meridional fashion. Their reactivity towards O<sub>2</sub> provides insight into the factors that tune the regiospecificity of cleavage.

The reactions of [(L)FeCl<sub>3</sub>], DBCH<sub>2</sub>, and NaOCH<sub>3</sub> in a 1:1:2 ratio in CH<sub>2</sub>Cl<sub>2</sub> under N<sub>2</sub> afforded complexes **1–3** as purple-black solids, which were recrystallized from THF/hexane, acetone, and DMF/Et<sub>2</sub>O, respectively. All of these complexes have high-spin iron(III) centers and exhibit two intense catecholate-to-iron(III) charge transfer bands in the spectral region of 400–1000 nm, similar to [(TPA)-Fe<sup>III</sup>(DBC)]BPh<sub>4</sub> (**4**).<sup>[3c]</sup> The crystal structures of **1** and **2** (Figure 1) reveal a distorted octahedral geometry with a facial (**1**) or meridional (**2**) tridentate ligand, a catecholate dianion, and a chloride ligand at the sixth coordination site.<sup>[6]</sup> The Fe–N and Fe–O bond lengths in both complexes are typical of high-spin iron(III) complexes. The fairly long Fe–Cl bond lengths (average 2.385(2) Å for **1** and 2.325(1) Å for **2**) suggest that the chloride ligand should be highly labile in solution.

Complexes **1–3** react with O<sub>2</sub> in the presence of one equivalent of AgOTf to afford oxidative cleavage products of DBC. The addition of silver salt removes the chloride ligand to generate an empty coordination site on the metal center and enhances the reactivity of the complex toward O<sub>2</sub>.<sup>[7]</sup> Complex **1**, with the *fac*-Me<sub>3</sub>TACN ligand, affords only

[\*] Prof. Dr. L. Que, Jr., Dr. D.-H. Jo

Department of Chemistry and Center for Metals in Biocatalysis  
University of Minnesota, Minneapolis, MN 55455 (USA)  
Fax: (+1) 612-624-7029  
E-mail: que@chem.umn.edu

[\*\*] This work was supported by a grant from the National Institutes of Health (GM-33162). D.-H.J. is grateful to the Korean Science and Engineering Foundation (KOSEF) for a postdoctoral fellowship. We thank Dr. Victor G. Young, Jr. and Dr. Maren Pink of the University of Minnesota X-ray Crystallographic Laboratory for determining the crystal structures of **1** and **2**.

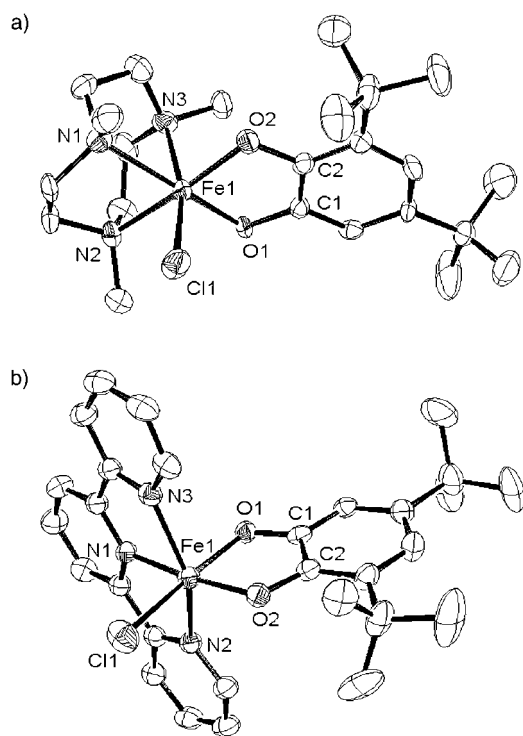


Figure 1. ORTEP plots for **1A** (a) and **2** (b) with hydrogen atoms omitted for clarity. The structure of **1B**, the other molecule in the asymmetric unit of **1**, is not shown. Selected bond lengths [Å] for **1A** and corresponding values for **1B** in brackets: Fe1–N1 [Fe2–N4] 2.226(6) [2.232(6)], Fe1–N2 [Fe2–N5] 2.202(6) [2.195(6)], Fe1–N3 [Fe2–N6] 2.276(6) [2.278(6)], Fe1–O1 [Fe2–O3] 1.941(4) [1.954(4)], Fe1–O2 [Fe2–O4] 1.920(5) [1.914(4)], Fe1–Cl1 [Fe2–Cl2] 2.381(2) [2.388(2)], O1–C1 [O3–C24] 1.361(8) [1.369(8)], O2–C2 [O4–C25] 1.366(8) [1.359(8)]. Selected bond lengths [Å] for **2**: Fe1–N1 2.137(2), Fe1–N2 2.143(2), Fe1–N3 2.173(3), Fe1–O1 1.990(2), Fe1–O2 1.913(2), Fe1–Cl1 2.325(1), O1–C1 1.329(3), O2–C2 1.343(9).

extradiol cleavage products (3,5- and 4,6-di-*tert*-butyl-2-pyrone) in nearly quantitative yield (97%). Previously, we reported that the TACN analogue of **1** also afforded extradiol cleavage products in nearly quantitative yield, but the addition of pyridine was needed to direct the reaction from simple auto-oxidation to form quinone to the desired cleavage.<sup>[4b, 8]</sup> Complex **2**, with the *mer*-TPY ligand, gives 3,5-di-*tert*-butyl-benzoquinone (78%) and the intradiol cleavage product 3,5-di-*tert*-butyl-1-oxacyclohepta-3,5-diene-2,7-dione (20%). Interestingly, **3** yields both extradiol (72%) and intradiol (25%) cleavage products. These results must be viewed in light of previously published papers which showed

that [(L)Fe<sup>III</sup>(DBC)] complexes with tetradentate ligands gave high yields of intradiol cleavage products (e.g., 98% for **4**).<sup>[3]</sup>

Table 1 summarizes the results for [(L)Fe<sup>III</sup>(DBC)] complexes reported thus far. The accumulated results show that the coordination geometry imposed by the ancillary ligand controls the regioselectivity of the oxidative cleavage reaction. Figure 2 shows a mechanistic scheme we propose to

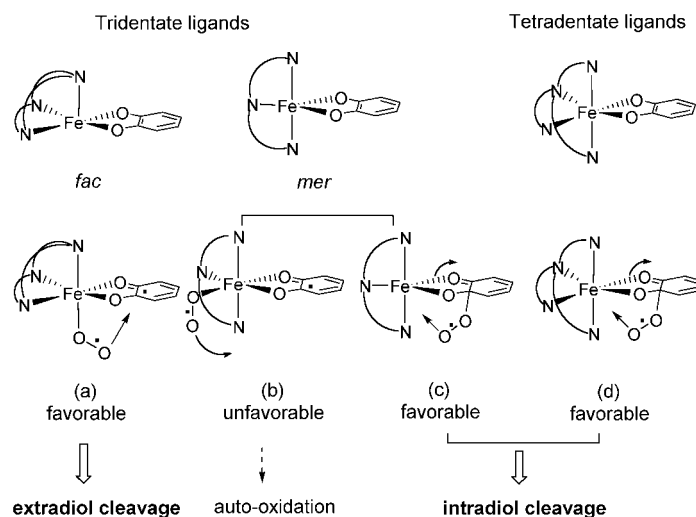


Figure 2. Proposed mechanism for the reaction of O<sub>2</sub> with [(L)Fe(DBC)] complexes.

rationalize the results. As discussed previously, the low energy of the catecholate-to-Fe<sup>III</sup> charge-transfer transitions confers an enhanced iron(II) semiquinonate character on the complexes, which is reflected in their spectroscopic properties.<sup>[3b, 3c]</sup> Thus two potential sites exist for interaction with O<sub>2</sub>: the metal center and the bound catecholate, and the nature of the products is determined by the initial site of O<sub>2</sub> attack. For [(L)Fe<sup>III</sup>(DBC)] complexes with tetradentate ligands, the metal center is coordinatively saturated, so O<sub>2</sub> attacks the catecholate to give rise to a bidentate peroxo intermediate that leads to intradiol cleavage, consistent with the mechanism of substrate activation proposed for intradiol-cleaving dioxygenases (Figure 2d).<sup>[1b,c]</sup> For complexes with tridentate ligands, the metal center has an available site for O<sub>2</sub> attack. For **1**, with the *fac*-Me<sub>3</sub>TACN ligand, only extradiol cleavage is observed. We propose that O<sub>2</sub> exclusively binds to the metal center and becomes activated to attack the bound

Table 1. Cleavage products obtained upon reaction of [(L)Fe<sup>III</sup>(DBC)] with O<sub>2</sub>.

L	Solvent	Intradiol [%]	Extradiol <sup>[a]</sup> [%]	Quinone [%]	Ref.
TACN	CH <sub>2</sub> Cl <sub>2</sub>	–	3	82	[4b]
TACN	CH <sub>3</sub> CN	–	35 (30/5)	65	[4a]
TACN + 20 equiv 4-picoline	CH <sub>2</sub> Cl <sub>2</sub>	–	98 (78/20)	trace	[4b]
Me <sub>3</sub> TACN	CH <sub>2</sub> Cl <sub>2</sub>	–	97 (83/14)	–	this work
TPY	CH <sub>2</sub> Cl <sub>2</sub>	20	–	78	this work
BnBPA	CH <sub>2</sub> Cl <sub>2</sub>	25	72 (62/10)	–	this work
Tp <sup>Pr2</sup>	toluene	33	67 (39/28)	–	[4c]
tetradentate ligands	DMF, CH <sub>3</sub> CN	84–98	–	–	[3a–e, h]

[a] Ratio in parentheses is that of 3,5- to 4,6-di-*tert*-butyl-2-pyrone.

catecholate. The facial nature of the ancillary ligand allows the two reactants to occupy the opposite face and form a tridentate peroxo intermediate that leads to extradiol cleavage (Figure 2a). This ideal geometry cannot be attained for **2**, a complex of the tridentate *mer*-TPY, which does not afford extradiol cleavage. Although O<sub>2</sub> can bind to the metal center in this complex, it is constrained to be in the same plane as the catecholate dianion, which it hence cannot attack (Figure 2b). Instead, the metal center acts as a conduit for electrons from substrate to O<sub>2</sub>, and this generates quinone (78%) as the major product. The minor amount of intradiol cleavage (20%) observed is due to the attack of O<sub>2</sub> on the bound substrate (Figure 2c). In the case of **3**, in which the tridentate BnBPA has the flexibility to act as a facial or meridional ligand, both intradiol and extradiol cleavage products are observed.<sup>[4c]</sup> The major extradiol cleavage product is formed by a mechanism analogous to that proposed for **1**, while the minor intradiol cleavage product results from attack of O<sub>2</sub> on bound substrate, as for the complexes with tetradentate ligands.

The above model studies show that a facial tridentate ancillary ligand is critical to elicit extradiol cleavage. In our proposed mechanism, the facial ligand allows O<sub>2</sub> and substrate to occupy the opposite face and form an intermediate that leads to the desired extradiol products. Such an intermediate may resemble the crystallographically characterized tridentate peroxo species derived from the reaction of catecholate complexes of iridium and rhodium with O<sub>2</sub>.<sup>[9]</sup> The facial tridentate ligand would then correspond to the common 2-His-1-carboxylate facial triad<sup>[10]</sup> found in the active sites of several extradiol dioxygenases, despite their having differing tertiary structures.<sup>[11]</sup> Our current model complexes are imperfect since they contain iron(III), not iron(II), centers; however, they do elicit the desired extradiol cleavage. We also do not yet understand how extradiol cleavage occurs once the key peroxo intermediate is formed. Attempts are in progress to trap this intermediate to gain further insight into the mechanism of this novel class of dioxygenase enzymes.

## Experimental Section

Syntheses of complexes: All Fe<sup>III</sup> catecholate complexes were prepared under nitrogen atmosphere. [(L)FeCl<sub>3</sub>] (1.0 mmol)<sup>[12]</sup> was dissolved in CH<sub>2</sub>Cl<sub>2</sub> (30 mL), and a solution of DBCH<sub>2</sub> (1.0 mmol) and NaOCH<sub>3</sub> (2.2 mmol) in CH<sub>2</sub>Cl<sub>2</sub> was slowly added. The mixture was stirred for 2 h, dried by evaporation in vacuo, then recrystallized from an appropriate solvent to give purple-black crystals. **1**: recrystallized from THF/hexane (yield 90%); elemental analysis calcd for **1**·0.5 THF (C<sub>25</sub>H<sub>45</sub>ClFeN<sub>3</sub>O<sub>2.5</sub>): C 57.86, H 8.74, N 8.10, Cl 6.83; found: C 57.96, H 8.65, N 8.20, Cl 7.03; electronic spectrum (CH<sub>3</sub>CN): λ<sub>max</sub> (ε) = 496 (1700), 820 nm (2100). **2**: recrystallized from CH<sub>2</sub>Cl<sub>2</sub>/Et<sub>2</sub>O and then DMF/Et<sub>2</sub>O (yield 60%); elemental analysis calcd for **2**·DMF (C<sub>32</sub>H<sub>38</sub>ClFeN<sub>4</sub>O<sub>3</sub>): C 62.19, H 6.20, N 9.07, Cl 5.90; found: C 61.85, H 6.23, N 8.98, Cl 5.44; electronic spectrum (CH<sub>3</sub>CN): λ<sub>max</sub> (ε) = 524 (1500), 830 nm (2100). **3**: recrystallized from acetone (yield 80%); elemental analysis calcd for **3** (C<sub>33</sub>H<sub>39</sub>ClFeN<sub>3</sub>O<sub>2</sub>): C 65.95, H 6.54, N 6.99, Cl 5.90; found: C 65.88, H 6.44, N 6.84, Cl 5.78; electronic spectrum (CH<sub>3</sub>CN): λ<sub>max</sub> (ε) = 520 (1200), 850 nm (2300).

Reactions with O<sub>2</sub>: 0.05 mmol of complex and AgOTf were dissolved in CH<sub>2</sub>Cl<sub>2</sub> (10 mL) and exposed to O<sub>2</sub> for 3 h. The solution was concentrated, and the organic products were extracted with diethyl ether (3 × 5 mL). The solid residue was then acidified with 3 N HCl to pH 3 to decompose the

metal complexes and extracted with diethyl ether (3 × 5 mL). The combined diethyl ether extracts were dried over anhydrous Na<sub>2</sub>SO<sub>4</sub>, concentrated, subjected to GC analysis (Hewlett-Packard 6890 Series gas chromatograph with a DB-5 column), and quantified by using 1,1'-biphenyl as internal standard.

Received: June 20, 2000 [Z 15304]

- [1] a) D. T. Gibson, *Microbial Degradation of Organic Molecules*, Marcel Dekker, New York, **1984**; b) J. D. Lipscomb, A. M. Orville, *Metal Ions Biol. Syst.* **1992**, 28, 243–298; c) L. Que, Jr. in *Bioinorganic Catalysis*, 2nd ed. (Eds.: J. Reedijk, E. Bouwman), Marcel Dekker, New York, **1999**, pp. 269–321; d) H.-J. Krüger in *Biomimetic Oxidations Catalyzed by Transition Metal Complexes* (Ed.: B. Meunier), Imperial College, London, **2000**, pp. 363–413.
- [2] L. Que, Jr., M. F. Reynolds, *Metal Ions Biol. Syst.* **2000**, 37, 505–525.
- [3] a) L. Que, Jr., R. C. Kolanczyk, L. S. White, *J. Am. Chem. Soc.* **1987**, 109, 5373–5380; b) D. D. Cox, L. Que, Jr., *J. Am. Chem. Soc.* **1988**, 110, 8085–8092; c) H. G. Jang, D. D. Cox, L. Que, Jr., *J. Am. Chem. Soc.* **1991**, 113, 9200–9204; d) W. O. Koch, H.-J. Krüger, *Angew. Chem.* **1995**, 107, 2928–2931; *Angew. Chem. Int. Ed. Engl.* **1995**, 34, 2671–2674; e) M. Duda, M. Pascaly, B. Krebs, *Chem. Commun.* **1997**, 835–836; f) T. Funabiki, T. Yamazaki, A. Fukui, T. Tanaka, S. Yoshida, *Angew. Chem.* **1998**, 110, 527–530; *Angew. Chem. Int. Ed.* **1998**, 37, 513–515; g) R. Viswanathan, M. Palaniandavar, T. Balasubramanian, T. P. Muthiah, *Inorg. Chem.* **1998**, 37, 2943–2951; h) P. Mialane, L. Tchertanov, F. Banse, J. Sainton, J.-J. Girerd, *Inorg. Chem.* **2000**, 39, 2440–2444.
- [4] a) A. Dei, D. Gatteschi, L. Pardi, *Inorg. Chem.* **1993**, 32, 1389–1395; b) M. Ito, L. Que, Jr., *Angew. Chem.* **1997**, 109, 1401–1403; *Angew. Chem. Int. Ed. Engl.* **1997**, 36, 1342–1344; c) T. Ogihara, S. Hikichi, M. Akika, Y. Moro-oka, *Inorg. Chem.* **1998**, 37, 2614–2615.
- [5] Abbreviations: BnBPA = *N*-benzyl *N,N*-bis(2-pyridylmethyl)amine; DBCH<sub>2</sub> = 3,5-di-*tert*-butylcatechol; Me<sub>3</sub>TACN = 1,4,7-trimethyl-1,4,7-triazacyclononane; TACN = 1,4,7-triazacyclononane; TPA = tris(2-pyridylmethyl)amine; Tp<sup>tr2</sup> = hydrotris(3,5-diisopropyl-1-pyrazolyl)-borate; TPY = 2,2':6',2''-terpyridine.
- [6] Crystal structure analysis: The data were collected on a Siemens SMART platform diffractometer equipped with a CCD detector (MoK<sub>α</sub> radiation; λ = 0.71073 Å). The structures were solved by direct methods and refined by full-matrix least-squares methods on *F*<sup>2</sup> by using the SHELXTL Plus program package (Version 5.1, Bruker Analytical X-Ray Systems, Madison, WI). All non-hydrogen atoms were refined with anisotropic thermal parameters, and all hydrogen atoms were placed in ideal positions and refined as riding atoms with individual isotropic displacement parameters. Crystal data for **1** at 173(2) K: C<sub>25</sub>H<sub>45</sub>ClFeN<sub>3</sub>O<sub>2.5</sub>, *M*<sub>r</sub> = 518.94, purple-black crystal of dimensions 0.6 × 0.38 × 0.08 mm, triclinic, space group *P* $\bar{1}$ , *a* = 13.0395(2), *b* = 15.5233(2), *c* = 16.7486(1) Å, α = 113.703(1), β = 111.192(1), γ = 92.132(1)°, *V* = 2827.35(6) Å<sup>3</sup>, *Z* = 4, ρ<sub>calcd</sub> = 1.219 g cm<sup>-3</sup>. On the basis of 9513 unique reflections (*R*<sub>int</sub> = 0.0572) and 633 variable parameters, final *R* values (*I* > 2σ(*I*)): *R*1 = 0.0787, *wR*2 = 0.1821. Crystal data for **2** at 173(2) K: C<sub>32</sub>H<sub>38</sub>ClFeN<sub>4</sub>O<sub>3</sub>, *M*<sub>r</sub> = 617.96, purple crystal of dimensions 0.40 × 0.12 × 0.05 mm, monoclinic, space group *P*2<sub>1</sub>/*c*, *a* = 12.3347(9), *b* = 13.552(11), *c* = 19.179(1) Å, α = 90, β = 97.426(2), γ = 90°, *V* = 3197.1(4) Å<sup>3</sup>, *Z* = 4, ρ<sub>calcd</sub> = 1.291 g cm<sup>-3</sup>. On the basis of 7190 unique reflections (*R*<sub>int</sub> = 0.0393) and 409 variable parameters, final *R* values (*I* > 2σ(*I*)): *R*1 = 0.0512, *wR*2 = 0.1450. Crystallographic data (excluding structure factors) for the structures reported in this paper have been deposited with the Cambridge Crystallographic Data Centre as supplementary publication no. CCDC-145996 (**1**) and CCDC-145997 (**2**). Copies of the data can be obtained free of charge on application to CCDC, 12 Union Road, Cambridge CB21EZ, UK (fax: (+44) 1223-336-033; e-mail: deposit@ccdc.cam.ac.uk).
- [7] Without AgOTf, the reactions require at least 24 h for completion but afford similar cleavage products.
- [8] Given that **1** affords nearly quantitative extradiol cleavage without the addition of pyridine, we do not currently understand the role that pyridine plays in the cleavage reaction with the TACN complex.

Clearly more work needs to be done on the apparently more complex TACN system.

- [9] a) P. Barbaro, C. Bianchini, K. Linn, C. Mealli, A. Meli, F. Vizza, *Inorg. Chim. Acta* **1992**, 198–200, 31–56; b) S. Dutta, S.-M. Peng, S. Bhattacharya, *Inorg. Chem.* **2000**, 39, 2231–2234.
- [10] a) S. Han, L. D. Eltis, K. N. Timmis, S. W. Muchmore, J. T. Bolin, *Science* **1995**, 270, 976–980; b) T. Senda, K. Sugiyama, H. Narita, T. Yamamoto, K. Kimbara, M. Fukuda, M. Sato, K. Yano, Y. Mitsui, *J. Mol. Biol.* **1996**, 255, 735–752; c) A. Kita, S.-I. Kita, I. Fujisawa, K. Inaka, T. Ishida, K. Horiike, M. Nozaki, K. Miki, *Structure* **1999**, 7, 25–34; d) K. Sugimoto, T. Senda, H. Aoshima, E. Masai, M. Fukuda, Y. Mitsui, *Structure* **1999**, 7, 953–965.
- [11] a) E. L. Hegg, L. Que, Jr., *Eur. J. Biochem.* **1997**, 250, 625–629; b) L. Que, Jr., *Nature Struct. Biol.* **2000**, 7, 182–185.
- [12] K. Wieghardt, K. Pohl, W. Gebert, *Angew. Chem.* **1983**, 95, 739–740; *Angew. Chem. Int. Ed. Engl.* **1983**, 22, 727.

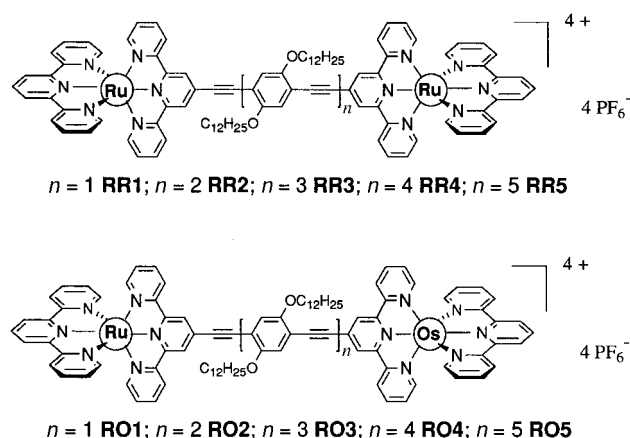
## An Unusually Shallow Distance-Dependence for Triplet-Energy Transfer\*\*

Anthony Harriman,\* Abderrahim Khatyr,  
Raymond Ziessel,\* and Andrew C. Benniston

There have been several reports of how the rate of intramolecular electron transfer<sup>[1]</sup> or triplet-energy transfer by electron exchange<sup>[2]</sup> decreases with increased separation of the reactants and, in many cases, an attenuation factor ( $\beta$ ) describing an exponential drop-off has been noted. The attenuation factor, which is often better expressed in terms of the number of interspersed repeat units rather than distance,<sup>[3]</sup> has values ranging from around 0.05 to 1.7 Å<sup>−1</sup> according to the nature of the connecting framework and the process under investigation.<sup>[4]</sup> It is recognized that the concept of an exponential-type attenuation factor applies only to those reactions that occur by way of superexchange<sup>[3]</sup> and, in other cases, the distance dependence might take on a different form.<sup>[5]</sup> With regard to triplet-energy transfer, this latter requisite demands that the transfer process involves electron exchange rather than dipole–dipole interactions. It is also important to ensure that the triplet energy of the interspersed connector unit does not fall below that of the donor triplet.

This realization presents a particular problem with regard to the construction of long bridges from conjugated subunits where, as happens for polyacetylenes,<sup>[6]</sup> the triplet energy of the connector decreases with increasing length. In such cases, long-range triplet energy transfer will be replaced by sequential short-range steps that give a deceptively small  $\beta$  value.<sup>[7]</sup> Herein we report that superexchange-type behavior is retained over more than 50 Å when the polyacetylene is doped with phenylene groups. This system provides an unusually small attenuation factor for triplet energy transfer.<sup>[8, 9]</sup>

The required set of heterodinuclear complexes (Scheme 1), comprising ruthenium(II) and osmium(II) bis(2,2':6',2''-terpyridine) terminals separated by a 1,4-diethynylene-2,5-dialkoxybenzene connector, was prepared in a two-step procedure.



Scheme 1. The dinuclear Ru<sup>II</sup>-based complexes and the corresponding mixed-metal Ru<sup>II</sup>/Os<sup>II</sup> complexes.

First, the soluble polytopic ligands were treated with [Ru(terpy)(dmsO)Cl<sub>2</sub>]<sup>[10]</sup> (terpy = 2,2':6',2''-terpyridine), dehalogenated with silver, in a mixture of dichloromethane and methanol to give the corresponding mono-Ru<sup>II</sup> complexes in 54 to 81% yield. These complexes, which contain an uncoordinated terpy fragment, were subsequently treated with [Os(terpy)(O)<sub>2</sub>(OH)](NO<sub>3</sub>)·2H<sub>2</sub>O in aqueous tetrahydrofuran using excess hydrazine hydrate as reducing agent.<sup>[4]</sup> The resultant mixed-metal Ru/Os hybrids were precipitated as PF<sub>6</sub><sup>−</sup> salts and purified by column chromatography on alumina prior to recrystallization from dichloromethane/hexane. Characterization was made by full spectroscopic and elemental analyses, including FAB<sup>+</sup> mass spectra which exhibited a molecular ion peak with the expected isotopic distributions and no significant peaks at higher mass. The corresponding dinuclear ruthenium(II) complexes were prepared according to a similar protocol using a slight excess of the metal precursor. Synthesis of the rationally designed polytopic ligands requires an iterative strategy based on palladium-promoted cross-coupling reactions to extend the central spacer framework outwards from the 1,4-diethynylene-2,5-diiododecyloxybenzene core.<sup>[11]</sup>

Photophysical properties for the dinuclear ruthenium(II) complexes were recorded in deoxygenated acetonitrile at 20 °C following excitation at 532 nm. In particular, the luminescence maxima ( $\lambda_{\text{MAX}}$ ), quantum yields ( $\Phi_{\text{LUM}}$ ), and lifetimes ( $\tau_{\text{LUM}}$ ) were as expected for an alkynylene-substi-

[\*] Prof. A. Harriman  
Department of Chemistry  
University of Newcastle  
Newcastle-upon-Tyne, NE1 7RU (UK)  
Fax: (+44)191-222-8664  
E-mail: Anthony.Harriman@newcastle.ac.uk

Dr. R. Ziessel, A. Khatyr  
Laboratoire de Chimie  
d'Electronique et de Photonique Moléculaires, Ecole Chimie  
Polymères, Matériaux (ECPM)  
UPRES-A 7008 au CNRS 25 rue Becquerel  
67087 Strasbourg Cedex (France)  
Fax: (+33)388-13-68-95  
E-mail: ziessel@chimie.u-strasbg.fr

Dr. A. C. Benniston  
Department of Chemistry, University of Glasgow, Glasgow G12 8QQ (UK)

[\*\*] This work was supported by the Centre National de la Recherche Scientifique and by the Engineering School of Chemistry (ECPM). We thank Prof. George Wipff (ULP) for many helpful discussions.